reason was probably due to misalignment of the electron gun. Output power levels were found to be comparable to that obtained with the old electron gun.

VI. Conclusions

A new cylindrical gun has been developed for a low-power tunable gyrotron. In this gun, the electrons are emitted axially rather than radially as in a conventional MIG. Transverse motion of the electrons is caused by the small radial component of the accelerating electric field.

A gun like this would be suitable for any gyrotrons which have very high magnetic compression ratios. Such high-compression ratios may arise in situations like ours where a small electron beam is required. Although the velocity spread in this gun is rather high, for fixed-frequency operations, the electron-beam quality could be improved further by optimization of the anode geometry [12].

The new gun has been tested successfully in a tunable gyrotron and has produced frequencies ranging from 93 to 250 GHz. Controllable and stable operation was possible throughout the whole range of frequencies.

The simple geometry of the cylindrical gun would perhaps allow a grid to be added to make the gun operate in a space-charge limited fashion. A space-charge limited gun would enable the current to be adjusted more readily to control the output power level; this is an advantage to a low-power source for spectroscopic purposes.

Acknowledgment

The author would wish to thank the Beijing Vacuum Electron Devices Research Institute for fabrication of the electron gun. He also acknowledges helpful suggestions from L. C. Robinson, G. F. Brand, and Z. Y. Chen. Special thanks are due to R. G. Hewitt for his advice on the computer simulations. The author would also like to thank colleagues of the gyrotron group for the experimental testing of the electron gun.

References

[1] H R. Jory, "Development of gyrotron power sources in the millimeter wavelength range," in *Proc. Joint Varenna-Grenoble Int. Symp. on Heating in Toroidal Plasmas* (Grenoble, France), July 1978, pp. 351–362

[2] A. V. Gaponov, V. A Flyagin, A. L. Gol'denberg, G. S Nusinovich, Sh. E. Tsimring, V. G. Usov, and S. N. Vlasov, "Powerful millimeter-wave gyrotrons," *Int. J. Electron*, vol. 51, no. 4, pp 277–302, 1981.

[3] Special issue on gyrotrons, *Int. J. Electron*, vol. 53, no. 6, 1982.

[4] M. Caplan and C. Thorington, "Improved computer modelling of magnetron injection gun for gyrotrons," *Int. J. Electron.*, vol. 51, no. 4, pp. 415–426, 1981.

[5] A. W. Fliflet, A. J. Dudas, M. E. Read, and J. M. Baird, "Use of electrode synthesis technique to design MIG-type guns for high power gyrotrons," *Int. J. Electron.*, vol. 53, no. 6, pp. 743–754, 1982.

[6] A. L Gol'denberg and M. I. Petelin, "The formation of helical electron beams in an adiabatic gun," *Radio Phys., Quantum Electron.*, vol. 16, no. 1, pp. 106–111, 1973.

[7] J. D. Jackson, *Classical Electrodynamics* New York: Wiley, 1975, p. 588.

[8] A. L. Gol'denberg and T. B. Pankratova, "Adiabatic theory of electron guns for CRM," (in Russian), *Elektronnaya Tekhnika*, ser. 1, Elektronika SVCh, no. 9, 1971

[9] G. F. Brand, N. G. Douglas, M. Gross, J Y. L. Ma, L. C Robinson, and Chen Zhiyi, "Tunable millimetre-wave gyrotrons," *Int. J. Infrared and Millimeter Waves*, vol. 3, no. 5, pp. 725–734, 1982.

[10] K. E. Kreischer and R. J Temkin, "Linear theory of an electron cyclotron maser operating at the fundamental," *Int. J. Infrared and Millimeter Waves*, vol. 1, no. 2, pp. 195–223, 1980.

[11] G. F. Brand, N. G. Douglas, M. Gross, J. Y. L. Ma, L. C. Robinson, and Chen Zhiyi, "A 125–260-GHz gyrotron," *IEEE Trans. Microwave Theory Tech.*, vol. MTT-32, pp. 58–64, Jan. 1984.

[12] V K. Lygin and Sh. E. Tsimring, "Electron trajectories in helical beams," *Soviet Physics–Technical Physics*, vol 16, no. 11, pp. 1809–1815, Nov 1971.

Probe Mutual Impedance in a Rectangular Waveguide

A. ITTIPIBOON, MEMBER IEEE, AND L. SHAFAI, SENIOR MEMBER IEEE

Abstract —**The mutual impedance between two probes, arbitrarily located on the broad walls of a rectangular waveguide, is derived by using the reaction concept. This mutual impedance is found to depend on the location and height of the probes and their separation distance. For probes of equal height, it reduces to the probe self impedance, as the probe separation distance approaches zero. The convergence of the solution and the effects of a terminating short circuit on the mutual impedance are also studied and discussed.**

I. Introduction

The problem of post-like structures in a waveguide have been studied by many investigators [1]–[5] who were interested in their equivalent impedance. The equivalent circuits represent a powerful tool for investigation and design of microwave circuits, matching transitions, and various filters. The couplings between waveguide obstacles were studied by Gruenberg [6] for posts of length equal to a waveguide height symmetrically located in the same transverse plane, by Chang and Khan [7] for unsymmetrical cases for posts without gaps, and by El-Sayed [8] for unsymmetrical cases for posts with gaps by using the variational principle. The problem of multipost of the same length equal to a waveguide height and with a gap in each post was studied by Joshi and Cornick [9]–[10]. The structure was considered as a linear N-port network with an impedance matrix obtained by applying the reaction concept. In the present investigation, we are mainly interested in the coupling between two probes arbitrarily located on the broad walls of a waveguide propagating only the dominant mode. The probe impedance as seen by the probe was previously obtained by Lewin [1], [11] and by Collin [12]; however, in this paper, the mutual impedance is obtained by applying the reaction concept [13]. Since the problem in a waveguide is eqivalent to the problem of an antenna radiating in a closed space, the radiation field of the probe can be expanded in terms of the eigenfunctions which form the solution space of the region under consideration. In the present case, the fields will be expanded in terms of the rectangular waveguide modes. The method is general and can be used to solve similar problems in waveguides of different cross sections by selecting their respective eigenfunctions.

Manuscript received August 8, 1984; revised November 13, 1984. This work was supported in part by a grant from the Natural Sciences and Engineering Research Council of Canada.

The authors are with the Department of Electrical Engineering, University of Manitoba, Canada R3T 2N2

0018-9480/85/0400-0327$01.00 ©1985 IEEE

drical reflector antenna. The input or received power is through one end of a waveguide while the other end is terminated in a short circuit or matched termination. The power is coupled to or from a waveguide to the line-source radiators through a large number of probes along the waveguide. The required aperture distribution of the line source can be obtained by properly adjusting the probe penetration into the waveguide which can be calculated by treating the problem as a linear N-port network. Hence, it is necessary that the probe mutual impedance is known.

II. Mutual Impedance Analysis

The probe antennas to be analyzed are shown in Fig. 1. The two probes are arbitrarily located on either the same or opposite faces of the broad side of a rectangular waveguide which propagates only the dominant mode. The probe diameter is assumed to be very small, as compared to waveguide dimensions, so that the surface current is angular-independent and can be represented by a current filament. The input region of the probe is considered as a small region of the probe having the property of causing a voltage drop ZI, when a current I flows at the input end of the probe.

By the reaction concept [13], the mutual impedance between the two probes is given by

$$Z_{21}=\frac{(-1)}{I_1(0)I_2(0)}\langle \boldsymbol{E}_1,\boldsymbol{I}_2\rangle=\frac{(-1)}{I_1(0)I_2(0)}\int \boldsymbol{E}_1\cdot \boldsymbol{I}_2\,dx \tag{1}$$

where $I_1(0)$ and $I_2(0)$ are the input currents at the first and second probes, respectively, $\boldsymbol{E}_1$ is the radiation field of the first probe at the location of the second probe in its absence, and $\boldsymbol{I}_2$ is the current distribution on the second probe.

By the reciprocity theorem we have

$$\langle \boldsymbol{E}_1,\boldsymbol{I}_2\rangle=\langle \boldsymbol{E}_2,\boldsymbol{I}_1\rangle. \tag{2}$$

Hence

$$Z_{21}=Z_{12}. \tag{3}$$

The exact current distribution on a probe can be obtained by the similar technique as given by Lewin [1]. The integral equation for the current distribution on the probe can be solved by the eigenfunction expansion technique or by the moment method. However, it can be shown that the mutual impedance given in (1) is stationary [13] which implies that a first-order approximation for the current gives a second-order approximation for the impedance. The simple form of the current distribution which has been successfully used by Collin [12] and Harrington [13] is given by

$$\begin{aligned}\mathbf{I}&=\hat{a}_x I_0\sin k_0(d-x)\,\delta(y-y'), && x\leqslant d\\ &=0, && x>d\end{aligned} \tag{4}$$

where d is the probe height and $\delta(y-y')$ is the Dirac-delta function representing the probe location at y' along the y-axis. The current distribution as given in (4) will be used in the following analysis.

A. Radiation Field of the First Probe

The mutual impedance Z_{21} as given in (1) can be calculated when the radiation field $\boldsymbol{E}_1$ of the first probe at the second probe is known. Since the region under consideration is a rectangular waveguide, the radiation field of the first probe can be represented by the summation of the TE and TM modes of the rectangular waveguide. However, instead of using the usual TE and TM to the z-axis modes, an alternative mode that sets TE and TM to the x-axis will be used. Since the probe current is in

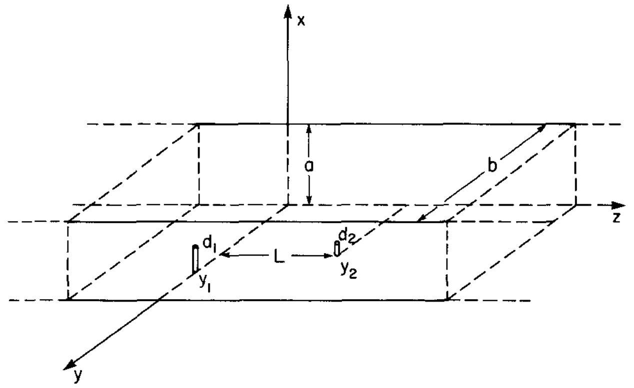

Fig. 1. Schematic diagram of probe antennas in a rectangular waveguide.

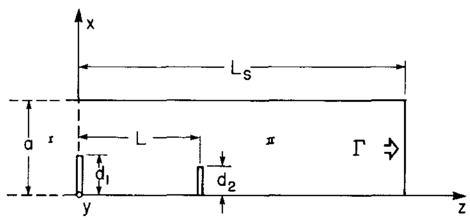

Fig. 2. Longitudinal section of a waveguide with two probes located on the same broad wall

the x-direction, only TM_x modes are excited. The dominant mode TM_{x01} is equivalent to TE_{z01}.

The structure under consideration is shown in Fig. 2 where region I, $z\leqslant 0$, is match-terminated, while region II, $z\geqslant 0$, is terminated at $z=L_s$ to a load with a reflection coefficient Γ. The first probe of height d_1 is located at $z=0$ and $y=y_1$. The current distribution on the first probe is given by

$$\begin{aligned}\boldsymbol{I}_1&=\hat{a}_x I_1\sin k_0(d_1-x)\,\delta(y-y_1), && x\leqslant d_1\\ &=0, && x>d_1.\end{aligned} \tag{5}$$

The field components in regions I and II can be obtained from the vector potentials $\boldsymbol{A}$ $(=\hat{a}_x\psi)$ with ψ satisfying the scalar Helmholtz equation in each region. After applying the boundary conditions which require the continuity of the tangential fields E_x and E_y, and

$$H_y^{\rm I}-H_y^{\rm II}=I_1\sin k_0(d_1-x)\,\delta(y-y_1). \tag{6}$$

The field components in regions I and II, with the time variation $e^{j\omega t}$ suppressed throughout, can be written as

$$E_x=\frac{1}{j\omega\epsilon}\sum_{m=0}^{\infty}\sum_{n=1}^{\infty}\left[k_0^2-\left(\frac{m\pi}{a}\right)^2\right]\cdot A_{mn}\cos\left(\frac{m\pi}{a}x\right)\sin\left(\frac{n\pi}{b}y\right)e^{jk_z z} \tag{7a}$$

$$H_y=j\sum_{m=0}^{\infty}\sum_{n=1}^{\infty}k_z A_{mn}\cos\left(\frac{m\pi}{a}x\right)\sin\left(\frac{n\pi}{b}y\right)e^{jk_z z} \tag{7b}$$

in region I, while in region II

$$E_x=\frac{1}{j\omega\epsilon}\sum_{m=0}^{\infty}\sum_{n=1}^{\infty}\left[k_0^2-\left(\frac{m\pi}{a}\right)^2\right]B_{mn}\left[e^{-jk_z z}+\Gamma e^{jk_z(z-2L_s)}\right]\cdot\cos\left(\frac{m\pi}{a}x\right)\sin\left(\frac{n\pi}{b}y\right) \tag{8a}$$

$$H_y = -j \sum_{m=0}^{\infty} \sum_{n=1}^{\infty} k_z B_{mn} \left[e^{-jk_z z} - \Gamma e^{jk_z(z-2L_s)} \right] \cdot \cos\left(\frac{m\pi}{a}x\right) \sin\left(\frac{n\pi}{b}y\right) \quad (8b)$$

where

$$k_z = \left\{ k_0^2 - \left(\frac{m\pi}{a}\right)^2 - \left(\frac{n\pi}{b}\right)^2 \right\}^{1/2} = -j\beta_{mn} \quad (9)$$

$$A_{mn} = B_{mn}\{1 + \Gamma e^{-j2k_z L_s}\} \quad (10)$$

$$A_{mn} = \frac{2I_1(1+\Gamma e^{-j2k_z L_s})}{jk_z ab\epsilon_m} \sin\left(\frac{n\pi}{b}y_1\right) g_m \quad (11)$$

$$\epsilon_m = 2, \quad m = 0; \qquad =1, \quad m \geqslant 1 \quad (12)$$

$$g_m = \frac{k_0}{\left[k_0^2 - \left(\frac{m\pi}{a}\right)^2\right]} \left[\cos\left(\frac{m\pi}{a}d_1\right) - \cos k_0 d_1\right]. \quad (13)$$

B. Mutual Impedance Calculation

Let the second probe of height d_2 be located at $y = y_2$ and at a distance $z = L$ from the first probe. The current distribution of the second probe is given by

$$\boldsymbol{I}_2 = \hat{a}_x I_2 \sin k_0(d_2 - x)\,\delta(y - y_2), \quad x \leqslant d_2; \qquad = 0, \quad x > d_2. \quad (14)$$

From (1), we have

$$Z_{21} = \frac{(-1)}{I_1(0)\,I_2(0)} \int_0^{d_2} E_{x1} I_2(x)\,dx. \quad (15)$$

Substituting $I_2(x)$ from (14) and E_{x1} from (8a) with $z = L$, we have after some simplifications

$$Z_{21} = \frac{2\eta_0 k_0}{ab} \tan\left(\frac{k_0 d_1}{2}\right) \tan\left(\frac{k_0 d_2}{2}\right) \cdot \sum_{m=0}^{\infty}\sum_{n=1}^{\infty} \frac{1}{k_z \epsilon_m \left[k_0^2 - \left(\frac{m\pi}{a}\right)^2\right]} \cdot \left[1 - \frac{\sin^2\left(\frac{m\pi}{2a}d_1\right)}{\sin^2\left(\frac{k_0 d_1}{2}\right)}\right]\left[1 - \frac{\sin^2\left(\frac{m\pi}{2a}d_2\right)}{\sin^2\left(\frac{k_0 d_2}{2}\right)}\right] \cdot \left(e^{-jk_z L} + \Gamma e^{jk_z(L-2L_s)}\right) \cdot \sin\left(\frac{n\pi}{b}y_1\right)\sin\left(\frac{n\pi}{b}y_2\right) \quad (16)$$

where $\eta_0 = \sqrt{\mu/\epsilon}$.

For real Γ, it is clear from the above equation that the mutual resistance R_{21} is mainly from the dominant mode $m = 0$ and $n = 1$ and is given by

$$R_{21} = \mathrm{Re}(Z_{21}) = \frac{\eta_0}{abk_{z0}k_0} \tan\left(\frac{k_0 d_1}{2}\right)\tan\left(\frac{k_0 d_2}{2}\right) \cdot \left[\cos(k_{z0}L) + \Gamma\cos\{k_{z0}(L-2L_s)\}\right] \cdot \sin\left(\frac{\pi}{b}y_1\right)\sin\left(\frac{\pi}{b}y_2\right). \quad (17)$$

The mutual reactance, however, consists of the dominant and the higher order modes and is given by

$$X_{21} = \frac{-\eta_0}{ab} \tan\left(\frac{k_0 d_1}{2}\right)\tan\left(\frac{k_0 d_2}{2}\right) \cdot \Bigg[\frac{1}{k_{z0}k_0}\left(\sin(k_{z0}L) - \Gamma\sin\{k_{z0}(L-2L_s)\}\right) \cdot \sin\left(\frac{\pi}{b}y_1\right)\sin\left(\frac{\pi}{b}y_2\right) + 2k_0 \sum_{\substack{m=0 \\ mn\neq 01}}^{\infty}\sum_{n=1}^{\infty} \frac{1}{\beta_{mn}\epsilon_m\left[\left(\frac{m\pi}{a}\right)^2 - k_0^2\right]} \cdot \left(1 - \frac{\sin^2\left(\frac{m\pi}{2a}d_1\right)}{\sin^2\left(\frac{k_0 d_1}{2}\right)}\right)\left(1 - \frac{\sin^2\left(\frac{m\pi}{2a}d_2\right)}{\sin^2\left(\frac{k_0 d_2}{2}\right)}\right) \cdot \left(e^{-\beta_{mn}L} + \Gamma e^{\beta_{mn}(L-2L_s)}\right) \cdot \sin\left(\frac{n\pi}{b}y_1\right)\sin\left(\frac{n\pi}{b}y_2\right) \Bigg] \quad (18)$$

where

$$k_{z0} = \sqrt{k_0^2 - \left(\frac{\pi}{b}\right)^2}. \quad (19)$$

When L is large, the double summation in (18) converges very rapidly. However, when L is small, some modifications are required to improve the rate of the convergence.

C. Mutual Impedance When L Approaches Zero

When L approaches zero, the mutual resistance is still given by (17), while the mutual reactance in (18) can be modified to improve the rate of convergence of the double summation. After some modifications, the mutual reactance can be written as

$$X_{21} = \frac{\eta_0}{2\pi k_0 a} \tan\left(\frac{k_0 d_1}{2}\right)\tan\left(\frac{k_0 d_2}{2}\right) \cdot \Bigg[\frac{1}{2}\left(\ln 2\left\{\cosh\frac{\pi L}{b} - \cos\frac{\pi}{b}(y_1+y_2)\right\} - \ln 2\left\{\cosh\frac{\pi L}{b} - \cos\frac{\pi}{b}(y_1-y_2)\right\}\right) - 2e^{-(\pi/b)L}\sin\left(\frac{\pi}{b}y_1\right)\sin\left(\frac{\pi}{b}y_2\right) - \frac{2\pi}{k_{z0}b}\left(\sin(k_{z0}L) - \Gamma\sin\{k_{z0}(L-2L_s)\}\right)\sin\left(\frac{\pi}{b}y_1\right)\sin\left(\frac{\pi}{b}y_2\right) + \frac{2\pi}{b}\sum_{n=2,3,4}^{\infty}\left[\frac{e^{-\beta_{0n}L}}{\beta_{0n}} - \frac{be^{-(n\pi/b)L}}{\pi n}\right]\sin\left(\frac{n\pi}{b}y_1\right)\sin\left(\frac{n\pi}{b}y_2\right) - 2k_0^2\sum_{m=1}^{\infty}\frac{1}{k_m^2}\left(1 - \frac{\sin^2\left(\frac{m\pi}{2a}d_1\right)}{\sin^2\left(\frac{k_0 d_1}{2}\right)}\right)\left(1 - \frac{\sin^2\left(\frac{m\pi}{2a}d_2\right)}{\sin^2\left(\frac{k_0 d_2}{2}\right)}\right) \cdot \left(K_0\left\{k_m\left(L^2 + (y_1-y_2)^2\right)^{1/2}\right\} - K_0\left\{k_m\left(L^2+(y_1+y_2)^2\right)^{1/2}\right\}\right)\Bigg] \quad (20)$$

where

$$k_m = \left[\left(\frac{m\pi}{a}\right)^2 - k_0^2\right]^{1/2}. \tag{21}$$

The summations in (20) converge very rapidly since $\beta_{0n} \to n\pi/b$ as n increases and K_0 is the modified Bessel function of the second kind which decays very rapidly. The detail derivation of (20) is given in the Appendix. When the two probes are located on the same cross-sectional plane $L = 0$, but different locations, i.e., $y_1 \neq y_2$, the mutual reactance is

$$\begin{aligned} X_{21} = \frac{\eta_0}{2\pi k_0 a} \tan\left(\frac{k_0 d_1}{2}\right) \tan\left(\frac{k_0 d_2}{2}\right) \Bigg[& \frac{1}{2}\left(\ln 2\left\{1 - \cos\frac{\pi}{b}(y_1 + y_2)\right\} - \ln 2\left\{1 - \cos\frac{\pi}{b}(y_1 - y_2)\right\}\right) \\ & - 2\left(1 + \frac{\pi\Gamma}{k_{z0} b}\sin(2k_{z0}L_s)\right)\sin\left(\frac{\pi}{b}y_1\right)\sin\left(\frac{\pi}{b}y_2\right) \\ & + \frac{2\pi}{b}\sum_{n=2,3,4}^{\infty}\left[\frac{1}{\beta_{0n}} - \frac{b}{\pi n}\right]\sin\left(\frac{n\pi}{b}y_1\right)\sin\left(\frac{n\pi}{b}y_2\right) \\ & - 2k_0^2\sum_{m=1}^{\infty}\frac{1}{k_m^2}\left(1 - \frac{\sin^2\left(\frac{m\pi}{2a}d_1\right)}{\sin^2\left(\frac{k_0 d_1}{2}\right)}\right)\left(1 - \frac{\sin^2\left(\frac{m\pi}{2a}d_2\right)}{\sin^2\left(\frac{k_0 d_2}{2}\right)}\right) \\ & \cdot\left(K_0\{k_m|y_1 - y_2|\} - K_0\{k_m|y_1 + y_2|\}\right)\Bigg]. \end{aligned} \tag{22}$$

For the special case when two probes of equal height $d_1 = d_2$ are located at $y_1 = y_2 = b/2$ in a rectangular guide with short-circuit termination ($\Gamma = -1$), R_{21} from (17) is reduced to

$$R_{21} = \frac{2\eta_0}{abk_{z0}k_0}\sin^2 k_{z0}L_s \tan^2\frac{k_0 d_1}{2}. \tag{23}$$

X_{21} from (20) can also be further simplified. It can easily be shown as $L \to 0$ that

$$\begin{aligned} \frac{1}{2}\left(\ln 2\left\{\cosh\frac{\pi L}{b} - \cos\frac{\pi}{b}(y_1 + y_2)\right\} - \ln 2\left\{\cosh\frac{\pi L}{b} - \cos\frac{\pi}{b}(y_1 - y_2)\right\}\right) &= \frac{1}{2}\ln\left\{\frac{\cosh\frac{\pi L}{b} + 1}{\cosh\frac{\pi L}{b} - 1}\right\} \\ &\approx \ln\frac{2b}{\pi L} \end{aligned} \tag{24}$$

$$2e^{-\pi L/b}\sin\left(\frac{\pi}{b}y_1\right)\sin\left(\frac{\pi}{b}y_2\right) \approx 2\left(1 - \frac{\pi L}{b}\right) \tag{25}$$

$$\frac{2\pi}{k_{z0}b}\left(\sin(k_{z0}L) - \Gamma\sin\{k_{z0}(L - 2L_s)\}\right) \approx \frac{2\pi}{k_{z0}b}\left(k_{z0}L(1 + \cos 2k_{z0}L_s) - \sin 2k_{z0}L_s\right) \tag{26}$$

$$\sum_{n=2,3,4}^{\infty}\left[\frac{e^{-\beta_{0n}L}}{\beta_{0n}} - \frac{be^{-(n\pi/b)L}}{\pi n}\right]\sin^2\left(\frac{n\pi}{2}\right) = \sum_{n=3,5,7}^{\infty}\left[\frac{e^{-\beta_{0n}L}}{\beta_{0n}} - \frac{be^{-(n\pi/b)L}}{\pi n}\right].$$

This term can be approximated as [12]

$$\sum_{n=3,5,7}^{\infty}\left[\frac{e^{-\beta_{0n}L}}{\beta_{0n}} - \frac{be^{-(n\pi/b)L}}{\pi n}\right] \approx \frac{1}{2}\frac{k_0^2 b^3}{\pi^3}\sum_{n=3,5,7}^{\infty}\frac{1}{n^3} = 0.0259\frac{k_0^2 b^3}{\pi^3}. \tag{27}$$

Substituting (24)–(27) into (20), it is reduced to

$$\begin{aligned} X_{21} &= \frac{\eta_0}{2\pi k_0 a}\tan^2\left(\frac{k_0 d_1}{2}\right)\Bigg[\ln\left(\frac{2b}{\pi L}\right) - 2\left(1 - \frac{\pi L}{b}\right) - 2\frac{\pi L}{b}(1 + \cos(2k_{z0}L_s)) \\ &\qquad + \frac{2\pi}{k_{z0}b}\sin(2k_{z0}L_s) + 0.0518\frac{k_0^2 b^2}{\pi^2} - 2k_0^2\sum_{m=1}^{\infty}\left(1 - \frac{\sin^2\left(\frac{m\pi}{2a}d_1\right)}{\sin^2\left(\frac{k_0 d_1}{2}\right)}\right)^2\frac{K_0(k_m L)}{k_m^2}\Bigg] \\ &\approx \frac{\eta_0}{2\pi k_0 a}\tan^2\left(\frac{k_0 d_1}{2}\right)\Bigg[\ln\left(\frac{2b}{\pi L}\right) + 0.0518\frac{k_0^2 b^2}{\pi^2} + \frac{2\pi}{k_{z0}b}\sin 2k_{z0}L_s - 2\left(1 - \frac{\pi L}{b}\right) \\ &\qquad - 2k_0^2\sum_{m=1}^{\infty}\left(\frac{1 - \sin^2\left(\frac{m\pi}{2a}d_1\right)}{\sin^2\left(\frac{k_0 d_1}{2}\right)}\right)^2\frac{K_0(k_m L)}{k_m^2}\Bigg]. \end{aligned} \tag{28}$$

Equations (23) and (28) are approximately the same as the probe self-impedance obtained by Collin [12] when $L = r$. Similarly, this is also true for (23) and (22) when the second probe is approaching the first probe located at $y_1 = b/2$. Hence, it can be concluded that when two probes of equal height approach each other, the mutual impedance is approaching the self-impedance.

III. Mutual Impedance When Two Probes are on the Opposite Face

The problem considered in this section is similar to that in the previous section. The first probe location remains the same as in the previous case, but the second probe is located on the opposite

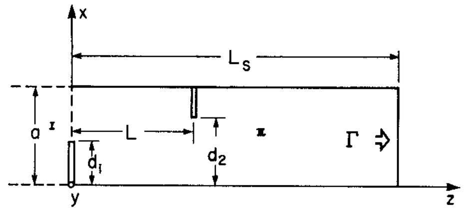

Fig. 3. Longitudinal section of a waveguide with two probes located on the opposite broad walls.

face, as shown in Fig. 3. The radiation field components of the first probe are still the same as those given in (7) and (8). The current distribution on the second probe is given by

$$I_2 = (-\hat{a}x) I_2 \sin k_0(x - d_2)\delta(y - y_2). \qquad (29)$$

Following the similar procedure as in the previous case, the mutual resistance and reactance are given by

$$R_{21} = \frac{-\eta_0}{abk_{z0}k_0} \tan\left(\frac{k_0 d_1}{2}\right) \tan\left\{\frac{k_0}{2}(a - d_2)\right\} \left(\cos(k_{z0}L) + \Gamma \cos\{k_{z0}(L - 2L_s)\}\right) \sin\left(\frac{\pi}{b}y_1\right) \sin\left(\frac{\pi}{b}y_2\right) \qquad (30)$$

$$X_{21} = \frac{\eta_0}{ab} \tan\left(\frac{k_0 d_1}{2}\right) \tan\left\{\frac{k_0}{2}(a - d_2)\right\} \cdot \left[\frac{1}{k_{z0}k_0}(\sin(k_{z0}L) - \Gamma \sin\{k_{z0}(L - 2L_s)\}) \cdot \sin\left(\frac{\pi}{b}y_1\right) \sin\left(\frac{\pi}{b}y_2\right) + 2k_0 \sum_{\substack{m=0 \\ mn \neq 01}}^{\infty} \sum_{n=1}^{\infty} \frac{1}{\epsilon_m \beta_{mn} k_m^2} \cdot \left(1 - \frac{\sin^2\left(\frac{m\pi}{2a}d_1\right)}{\sin^2\left(\frac{k_0 d_1}{2}\right)}\right) \left(1 + \frac{(-1)^{m+1} + 1 - 2\sin^2\left(\frac{m\pi}{2a}d_2\right)}{2\sin^2\left\{\frac{k_0}{2}(a - d_2)\right\}}\right) \cdot \left(e^{-\beta_{mn}L} + \Gamma e^{\beta_{mn}(L - 2L_s)}\right) \sin\left(\frac{n\pi}{b}y_1\right) \sin\left(\frac{n\pi}{b}y_2\right)\right]. \qquad (31)$$

The double summation in (31) is rapidly convergent for large values of L. As L approaches zero, (31) can be modified so that the series is still rapidly convergent. Hence, for small L, X_{21} is given by

$$X_{21} = \frac{-\eta_0}{2\pi k_0 a} \tan\left(\frac{k_0 d_1}{2}\right) \tan\left\{\frac{k_0}{2}(a - d_2)\right\} \cdot \left[\frac{1}{2}\left(\ln 2\left\{\cosh\frac{\pi L}{b} - \cos\frac{\pi}{b}(y_1 + y_2)\right\} - \ln 2\left\{\cosh\frac{\pi L}{b} - \cos\frac{\pi}{b}(y_1 - y_2)\right\}\right) - \frac{2\pi}{bk_{z0}}\left(\frac{bk_{z0}}{\pi}e^{-(\pi/b)L} + \sin(k_{z0}L) - \Gamma \sin\{k_{z0}(L - 2L_s)\}\right) \sin\left(\frac{\pi}{b}y_1\right) \sin\left(\frac{\pi}{b}y_2\right) + \frac{2\pi}{b} \sum_{n=2,3,4}^{\infty} \left[\frac{e^{-\beta_{0n}L}}{\beta_{0n}} - \frac{be^{-(n\pi/b)L}}{\pi n}\right] \cdot \sin\left(\frac{n\pi}{b}y_1\right) \sin\left(\frac{n\pi}{b}y_2\right) - 2k_0^2 \sum_{m=1,2,3}^{\infty} \frac{1}{k_m^2} \left(1 - \frac{\sin^2\left(\frac{m\pi}{2a}d_1\right)}{\sin^2\left(\frac{k_0 d_1}{2}\right)}\right) \cdot \left(1 + \frac{1 - (-1)^m - 2\sin^2\left(\frac{m\pi}{2a}d_2\right)}{2\sin^2\left\{\frac{k_0}{2}(a - d_2)\right\}}\right) \cdot \left(K_0\left\{k_m\left(L^2 + (y_1 - y_2)^2\right)^{1/2}\right\} - K_0\left\{k_m\left(L^2 + (y_1 + y_2)^2\right)^{1/2}\right\}\right)\right]. \qquad (32)$$

The summations in (32) converge very rapidly, since $\beta_{0n} \to n\pi/b$ for large n and K_0 is the modified Bessel function of the second kind, which decays very rapidly.

IV. Results

It was shown in the previous sections that the mutual impedance is dependent on the heights and locations of the two probes, along the width and length of the waveguide. The location of the terminating load can also influence the mutual impedance. It was also found that when the two probes of equal height approach each other, the mutual impedance is equal to the self impedance. Some of the numerical results are given below for the probe mutual impedance in the rectangular guide with $a = 0.4$ in, and $b = 0.9$ in at the operating frequency of 9.4 GHz.

The results of the mutual impedance against the probe separation distance L are shown in Figs. 4 and 5. The terminating load is a short circuit ($\Gamma = -1$) located at a distance $L_s = N\lambda_g/2 + l$ from the first probe where N is any integer and λ_g is the guide wavelength. It can be seen from (17), (20), and (22) for small L, that L_s always appears under $\cos k_{z0}(L - 2L_s)$ and $\sin k_{z0}(L - 2L_s)$, hence changing N does not change the mutual impedance. However, the mutual impedance can be changed by varying l. For large L, $e^{\beta_{mn}(L - 2L_s)}$ is usually negligible in (18) since L_s is always greater than L. The mutual resistance vanishes when $l = 0$, while the mutual reactance is maximum and oscillates with a period of λ_g. The major contribution to the mutual reactance is from the dominant mode, since the higher order modes decay rapidly with increasing L. However, as L approaches zero, the higher order modes are dominating, which results in a large value of the mutual reactance. As l increases toward $\lambda_g/4$, the mutual resistance increases while the mutual

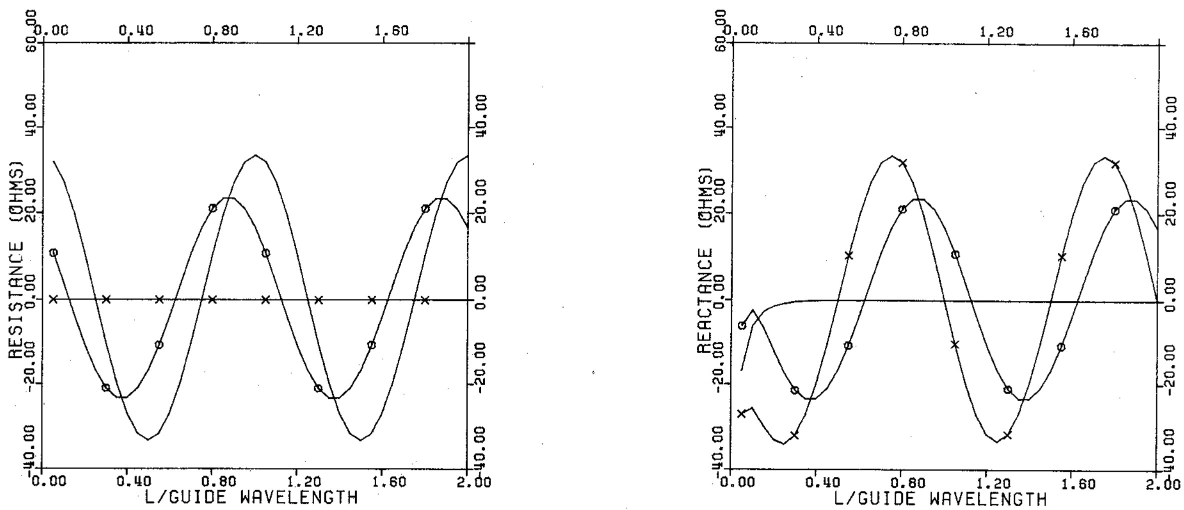

Fig. 4. The mutual impedance against probe separation distance for different L_s with $d_1 = d_2 = 0.492a$ and $y_1 = y_2 = b/2$. × × ×: $l = 0$, ○ ○ ○: $l = \lambda g/8$, ——: $l = \lambda g/4$.

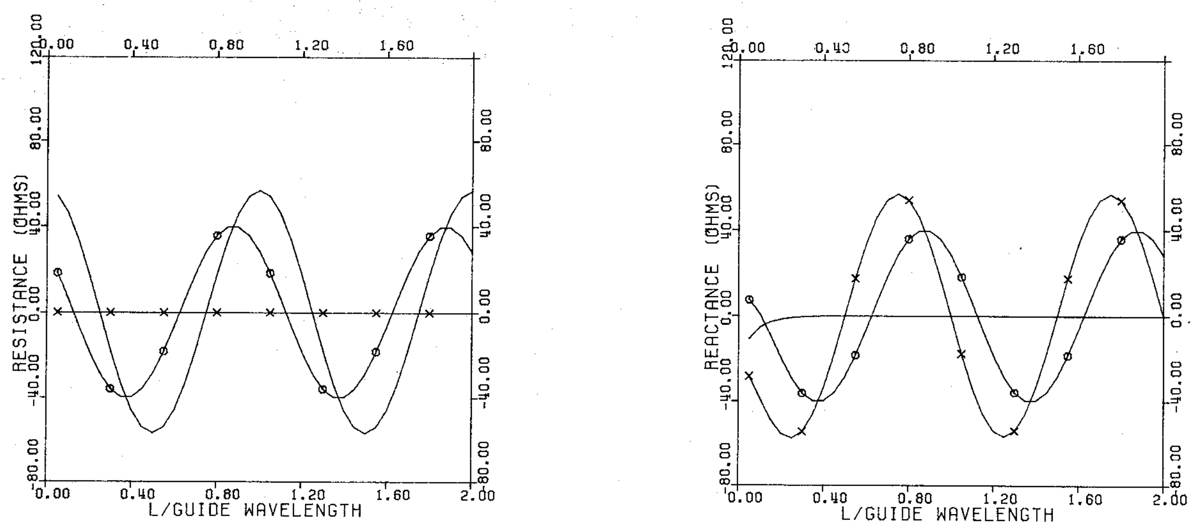

Fig. 5. The mutual impedance against probe separation distance for different L_s with $d_1 = 0.492a$, $d_2 = 0.738a$, and $y_1 = y_2 = b/2$. × × ×: $l = 0$, ○ ○ ○: $l = \lambda g/8$, ——: $l = \lambda g/4$.

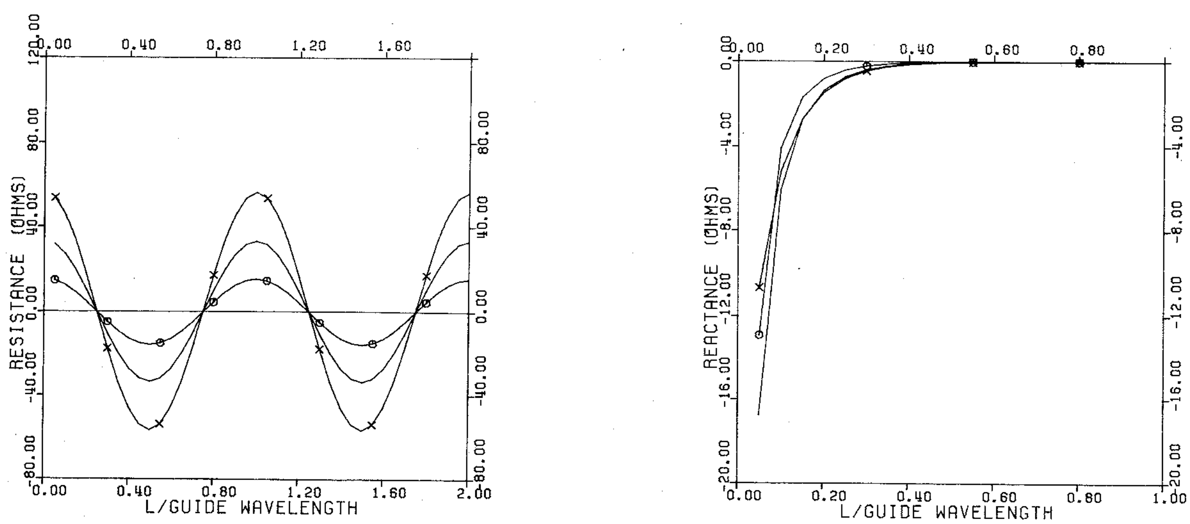

Fig. 6. The mutual impedance against probe separation distance for different second probe heights with $y_1 = y_2 = b/2$ and $d_1 = 0.492a$, $l = \lambda g/4$. ○ ○ ○: $d_2 = 0.246a$, ——: $d_2 = 0.492a$, × × ×: $d_2 = 0.738a$.

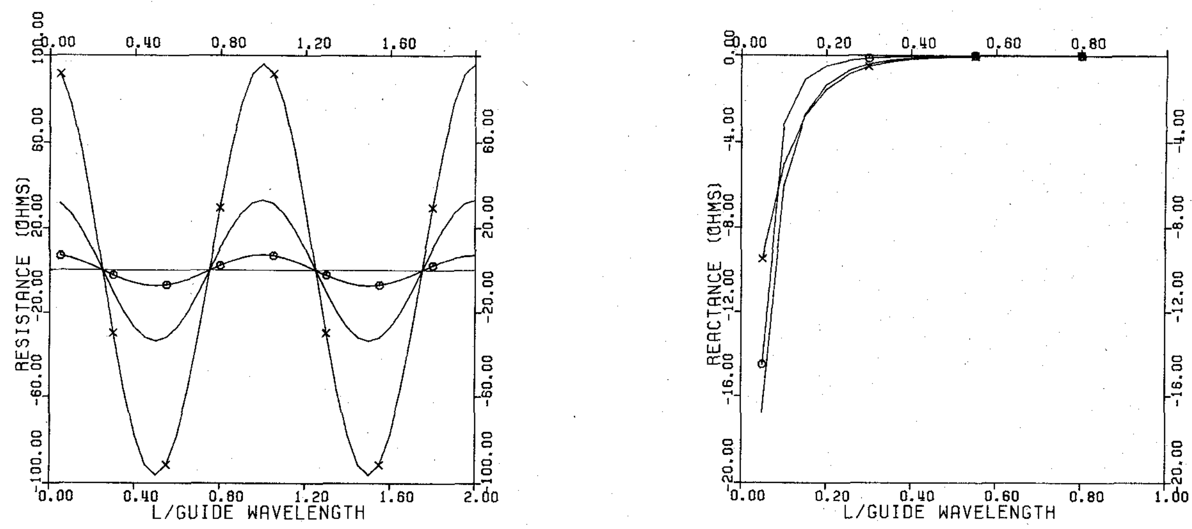

Fig. 7. The mutual impedance against probe separation distance for different probe heights with $y_1 = y_2 = b/2$, $l = \lambda g/4$. ○ ○ ○: $d_1 = d_2 = 0.246a$, ———: $d_1 = d_2 = 0.492a$, × × ×: $d_1 = d_2 = 0.738a$.

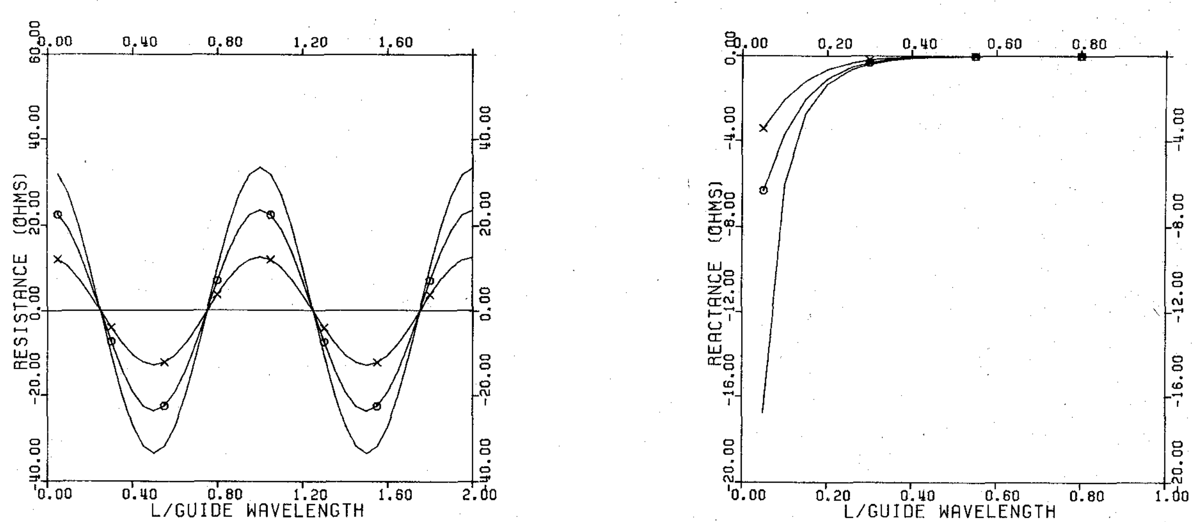

Fig. 8. The mutual impedance against probe separation distance for different probe locations with $d_1 = d_2 = 0.492a$, $l = \lambda g/4$. × × ×: $y_1 = b/2$, $y_2 = b/8$, ○ ○ ○: $y_1 = b/2$, $y_2 = b/4$, ———: $y_1 = b/2$, $y_2 = b/2$.

reactance decreases. At $l = \lambda_g/4$, the mutual resistance is maximum with the $\cos(k_{z0}L)$ variation. The contribution of the dominant mode to the mutual reactance vanishes, while that of the higher order modes decay very rapidly with increasing L. The mutual reactance is usually negligible, compared to the mutual resistance when $L \geqslant \lambda_g/4$.

The results of the mutual resistance and reactance when $L_s = N\lambda_g/2 + \lambda_g/4$ against L are shown in Figs. 6–8 for different probe heights and probe locations along the broad wall. In Figs. 6 and 7, both probes are located at the center of the broad wall, while the probe heights are used as variable parameters. In Fig. 8, the probe heights are kept constant, while the probe location along the broad wall is used as a variable parameter. It was found that the mutual resistance is always increased with the probe heights and it is maximum for any pair of probes if both probes are located at the center of the broad wall. The mutual reactance is very large for small probe separation L and it decreases very rapidly as L increases, since the major contribution to the mutual reactance is from the higher order modes. The mutual impedance decreases to zero when the probes are moved toward the side walls.

V. Conclusion

The mutual impedance between two probes located on the broad wall of a rectangular waveguide was derived by using the reaction concept. It was found that the mutual impedance is dependent on the probe heights, their locations, their separation distance, and the waveguide terminating load. The mutual impedance of the two equal height probes approaches the self impedance as the two probes approach each other. The contribution to the mutual resistance comes from the dominant mode, while the contribution to the mutual reactance comes from the dominant and the higher order modes. However, by properly adjusting the distance of the short-circuit termination, the contribution of the dominant mode to the mutual reactance can be eliminated, which results in a negligible mutual reactance when the probe separation is greater than a quarter guide wavelength.

The obtained results are applicable to the design of a line source with specific aperture distribution as a feed for a cylindrical parabolic reflector. The required distribution can be obtained by a proper design of probe penetration lengths. Since there is 180° phase difference for every probe located half a guide wavelength apart, the 180° phase reversal is required at every alternate probe to provide a uniform phase distribution.

Appendix
Derivation of (20)

As L approaches zero, the double summation over m and n in (18) can be modified to improve the rate of convergence. Rewriting the double summation in (18), we have

$$X_{21}'' = -\frac{2\eta_0 k_0}{ab}\tan\left(\frac{k_0 d_1}{2}\right)\tan\left(\frac{k_0 d_2}{2}\right) \cdot \sum_{\substack{m=0\\ mn\neq 01}}^{\infty}\sum_{n=1}^{\infty}\frac{1}{\beta_{mn}\epsilon_m\left[\left(\frac{m\pi}{a}\right)^2-k_0^2\right]} \cdot\left(1-\frac{\sin^2\left(\frac{m\pi}{2a}d_1\right)}{\sin^2\left(\frac{k_0 d_1}{2}\right)}\right)\left(1-\frac{\sin^2\left(\frac{m\pi}{2a}d_2\right)}{\sin^2\left(\frac{k_0 d_2}{2}\right)}\right) \cdot\left(e^{-\beta_{mn}L}+\Gamma e^{\beta_{mn}(L-2L_s)}\right) \cdot\sin\left(\frac{n\pi}{b}y_1\right)\sin\left(\frac{n\pi}{b}y_2\right). \tag{A1}$$

The term $\Gamma e^{\beta_{mn}(L-2L_s)}$ is negligible, since L_s is usually large. The double summation in (A1) is considered separately for $m=0$ and $m\geqslant 1$. For $m=0$, we have

$$\sum_n X_{0n} = \frac{\eta_0}{abk_0}\tan\left(\frac{k_0 d_1}{2}\right)\tan\left(\frac{k_0 d_2}{2}\right) \cdot\sum_{n=2,3,4}^{\infty}\frac{e^{-\beta_{0n}L}}{\beta_{0n}}\sin\left(\frac{n\pi}{b}y_1\right)\sin\left(\frac{n\pi}{b}y_2\right) \tag{A2}$$

where

$$\beta_{0n} = \left\{\left(\frac{n\pi}{b}\right)^2 - k_0^2\right\}^{1/2}. \tag{A3}$$

The summation over n in (A2) can be modified to improve the rate of convergence as

$$\sum_{n=2,3,4}^{\infty}\frac{e^{-\beta_{0n}L}}{\beta_{0n}}\sin\left(\frac{n\pi}{b}y_1\right)\sin\left(\frac{n\pi}{b}y_2\right) = -\frac{b}{\pi}e^{(-\pi/b)L}\sin\left(\frac{\pi}{b}y_1\right)\sin\left(\frac{\pi}{b}y_2\right) + \sum_{n=2,3}^{\infty}\left(\frac{e^{-\beta_{0n}L}}{\beta_{0n}}-\frac{be^{-(n\pi/b)L}}{\pi n}\right)\sin\left(\frac{n\pi}{b}y_1\right)\sin\left(\frac{n\pi}{b}y_2\right) + \frac{b}{\pi}\sum_{n=1,2,3}^{\infty}\frac{e^{-(n\pi/b)L}}{n}\sin\left(\frac{n\pi}{b}y_1\right)\sin\left(\frac{n\pi}{b}y_2\right). \tag{A4}$$

Applying [6]

$$\sum_{n=1}^{\infty}\frac{1}{n}e^{-np}\cos nq = \frac{1}{2}\left[p-\ln 2(\cosh p - \cos q)\right] \tag{A5}$$

and the trigonometric identity

$$\sin A \sin B = \frac{1}{2}\cos(A-B) - \frac{1}{2}\cos(A+B) \tag{A6}$$

we obtain

$$\frac{b}{\pi}\sum_{n=1,2,3}^{\infty}\frac{e^{-(n\pi/b)L}}{n}\sin\left(\frac{n\pi}{b}y_1\right)\sin\left(\frac{n\pi}{b}y_2\right) = \frac{b}{4\pi}\left[\ln 2\left\{\cosh\frac{\pi L}{b}-\cos\frac{\pi}{b}(y_1+y_2)\right\} + \ln 2\left\{\cosh\frac{\pi L}{b}-\cos\frac{\pi}{b}(y_1-y_2)\right\}\right]. \tag{A7}$$

Hence

$$\sum_{n=2,3,\ldots}^{\infty} X_{0n} = \frac{\eta_0}{abk_0}\tan\left(\frac{k_0 d_1}{2}\right)\tan\left(\frac{k_0 d_2}{2}\right) \cdot\left[\frac{b}{4\pi}\left(\ln 2\left\{\cosh\frac{\pi}{b}L-\cos\frac{\pi}{b}(y_1+y_2)\right\} - \ln 2\left\{\cosh\frac{\pi}{b}L-\cos\frac{\pi}{b}(y_1-y_2)\right\}\right) - \frac{b}{\pi}e^{-(\pi/b)L}\sin\left(\frac{\pi}{b}y_1\right)\sin\left(\frac{\pi}{b}y_2\right) + \sum_{n=2,3,4}^{\infty}\left(\frac{e^{-\beta_{0n}L}}{\beta_{0n}}-\frac{be^{-(n\pi/b)L}}{\pi n}\right) \cdot\sin\left(\frac{n\pi}{b}y_1\right)\sin\left(\frac{n\pi}{b}y_2\right)\right]. \tag{A8}$$

The summation in (A8) can also be further approximated for small n; however, since it is a rapidly convergent series, it has been left unmodified.

From $m\geqslant 1$, we have

$$\sum_{m=1}^{\infty}\sum_{n=1}^{\infty} X_{mn} = -\frac{\eta_0 k_0}{ab}\tan\left(\frac{k_0 d_1}{2}\right)\tan\left(\frac{k_0 d_2}{2}\right) \cdot\sum_{m=1,2}^{\infty}\frac{1}{k_m^2}\left(1-\frac{\sin^2\left(\frac{m\pi}{2a}d_1\right)}{\sin^2\left(\frac{k_0 d_1}{2}\right)}\right) \cdot\left(1-\frac{\sin^2\left(\frac{m\pi}{2a}d_2\right)}{\sin^2\left(\frac{k_0 d_2}{2}\right)}\right)\sum_{n=1,2,3}^{\infty}\frac{e^{-\beta_{mn}L}}{\beta_{mn}} \cdot\left(\cos\frac{n\pi}{b}(y_1-y_2)-\cos\frac{n\pi}{b}(y_1+y_2)\right) \tag{A9}$$

where

$$k_m^2 = \left(\frac{m\pi}{a}\right)^2 - k_0^2. \tag{A10}$$

The summation over n in (A9) can be transformed into a new series with a faster convergence. Let

$$f_1(\omega) = \frac{e^{-L(\omega^2+k_m^2)^{1/2}}}{(\omega^2+k_m^2)^{1/2}}. \tag{A11}$$

Its Fourier transform is given by

$$F_1(\alpha) = 2K_0\left\{k_m(L^2+\alpha^2)^{1/2}\right\} \tag{A12}$$

where K_0 is the modified Bessel function of the second kind. The Fourier transform of $f_2(\omega) = \cos \omega A_0$ is given by

$$F_2(\alpha) = \pi[\delta(\alpha - A_0) + \delta(\alpha + A_0)]. \tag{A13}$$

Using (A12) and (A13), the Fourier transform of $f_3(\omega) = f_1(\omega) f_2(\omega)$ can easily be found

$$F_3(\alpha) = K_0\left\{k_m\left(L^2 + (\alpha - A_0)^2\right)^{1/2}\right\} + K_0\left\{k_m\left(L^2 + (\alpha + A_0)^2\right)^{1/2}\right\}. \tag{A14}$$

Using (A14) in the Poisson summation formula

$$\sum_{n=-\infty}^{\infty} f_3\left(\frac{n\pi}{b}\right) = \frac{b}{\pi} \sum_{n=-\infty}^{\infty} F_3(2nb) \tag{A15}$$

after some algebraic manipulation we have

$$\begin{aligned}\sum_{n=1,2,3}^{\infty} \frac{e^{-\beta_{mn}L}}{\beta_{mn}} &\left(\cos\frac{n\pi}{b}(y_1 - y_2) - \cos\frac{n\pi}{b}(y_1 + y_2)\right) \\ &= \frac{b}{2\pi} \sum_{n=-\infty}^{\infty} \Big[K_0\left\{k_m\left(L^2 + (2nb - y_1 + y_2)^2\right)^{1/2}\right\} \\ &+ K_0\left\{k_m\left(L^2 + (2nb + y_1 - y_2)^2\right)^{1/2}\right\} \\ &- K_0\left\{k_m\left(L^2 + (2nb - y_1 - y_2)^2\right)^{1/2}\right\} \\ &- K_0\left\{k_m\left(L^2 + (2nb + y_1 + y_2)^2\right)^{1/2}\right\}\Big]. \end{aligned} \tag{A16}$$

The modified Bessel function of the second kind decays rapidly so that, as $L \to 0$, the only significant terms in (A16) are those for $n = 0$, hence

$$\begin{aligned}\sum_{n=1,2,3,}^{\infty} \frac{e^{-\beta_{mn}L}}{\beta_{mn}} &\left(\cos\frac{n\pi}{b}(y_1 + y_2) - \cos\frac{n\pi}{b}(y_1 + y_2)\right) \\ &\simeq \frac{b}{\pi}\Big[K_0\left\{k_m\left(L^2 + (y_1 - y_2)^2\right)^{1/2}\right\} \\ &- K_0\left\{k_m\left(L^2 + (y_1 + y_2)^2\right)^{1/2}\right\}\Big]. \end{aligned} \tag{A17}$$

Substituting (A17) into (A9), we have

$$\begin{aligned}\sum_{m=1}^{\infty}\sum_{n=1}^{\infty} X_{mn} = -\frac{\eta_0 k_0}{\pi a} &\tan\left(\frac{k_0 d_1}{2}\right) \tan\left(\frac{k_0 d_2}{2}\right) \\ &\cdot \sum_{m=1,2,}^{\infty} \left(1 - \frac{\sin^2\left(\frac{m\pi}{2a} d_1\right)}{\sin^2\left(\frac{k_0 d_1}{2}\right)}\right) \\ &\cdot \left(1 - \frac{\sin^2\left(\frac{m\pi}{2a} d_2\right)}{\sin^2\left(\frac{k_0 d_2}{2}\right)}\right) \frac{1}{k_m^2} \\ &\cdot \Big[K_0\left\{k_m\left(L^2 + (y_1 - y_2)^2\right)^{1/2}\right\} \\ &- K_0\left\{k_m\left(L^2 + (y_1 + y_2)^2\right)^{1/2}\right\}\Big]. \end{aligned} \tag{A18}$$

By substituting (A8) and (A18) into (18), (20) is obtained.

References

[1] L. Lewin, "A contribution to the theory of probes in waveguide," *Proc Inst. Elec. Eng.*, pt. C , vol. 105, pp. 109–116, 1958

[2] J. A. Bradshaw, "Scattering from a round metal post and gap." *IEEE Trans. Microwave Theory Tech* , vol. MTT-21, pp. 313–322, May 1973.

[3] S. L Lopuch and T. Koryuishii, "Field distribution of two conducting posts in a waveguide," *IEEE Trans. Microwave Theory Tech.*, vol. MTT-32, pp 29–33, Jan. 1984.

[4] O. L. El-Sayed, "Impedance characterization of a two-post mounting structure for varactor-tuned Gunn oscillators," *IEEE Trans Microwave Theory Tech.*, vol. MTT-22, pp. 769–776, Aug. 1974

[5] N Marcuvitz, *Waveguide Handbook*. New York: McGraw-Hill, ch. 5, 1951.

[6] H. Gruenberg, "Symmetrically placed inductive posts in rectangular waveguide," *Can J. Phys* , vol. 30, pp. 211–217, May 1952.

[7] K. Chang and P. J Khan, "Coupling between narrow tranverse inductive strips in waveguide," *IEEE Trans. Microwave Theory Tech.*, vol MTT-24, pp 101–105, Feb. 1976

[8] O. L. El-Sayed, "Generalized analysis of parallel two-post mounting structures in waveguide," *IEEE Trans. Microwave Theory Tech.*, vol MTT-25, pp. 24–33, Jan. 1977.

[9] J. S. Joshi and J. A. F. Cornick, "Analysis of waveguide post configurations: Part I—gap immittance matrices," *IEEE Trans. Microwave Theory Tech.*, vol. MTT-25, pp. 169–173, Mar. 1977.

[10] J. S Joshi and J. A. F. Cornick, "Analysis of waveguide post configurations: Part II—dual-gap cases," *IEEE Trans. Microwave Theory Tech* , vol. MTT-25, pp. 173–181, Mar. 1977

[11] L. Lewin, *Theory of Waveguide*. London: Newnes-Butterworths, ch 5, 1975.

[12] R. E. Collin, *Field Theory of Guided Waves*. New York: McGraw-Hill, ch. 7, Math. Appendix, 1960.

[13] R. F. Harrington, *Time Harmonic Electromagnetic Fields*. New York: McGraw-Hill, chs. 3, 7, 8, 1961.

[14] A W. Rudge, K. Milne, A. D. Olver, and P. Knight, Eds., *The Handbook of Antenna Design: Volume 2*. London: Peter Peregrinus Ltd., ch. 9, 1983.

Slow-Wave Propagation in Two Types of Cylindrical Waveguides Loaded with a Semiconductor

CLIFFORD M. KROWNE, SENIOR MEMBER, IEEE

Abstract—**For a parallel-plate waveguide and a microstripline loaded with a semiconductor slab of resistive (or active) character, the complex propagation constant γ is determined. γ is found for higher order branches for microwave and millimeter-wave frequencies between 10 and 140 GHz, representing a study of phase velocity slowing (and attenuation).**

I. Introduction

Slow-wave structures and devices are important because of the many applications to which they have been applied and to which they may be applied in the future. Applications using an electron–electromagnetic interaction include devices such as the solid-state traveling-wave amplifier, solid-state magnetron, distributed FET, and distributed amplifier. Applications using only the electromagnetic slowing effect include the variable phase shifter, voltage-tunable filter, delay line, and variable coupling coefficient directional coupler.

It is the intent of this paper to obtain an idea of the millimeter-wave slowing behavior of cylindrical waveguide structures loaded with a semiconductor slab. To accomplish this task, two structures are examined: a parallel-plate waveguide and a microstripline, both loaded by a dielectric–semiconductor two-

Manuscript received August 16, 1983; revised November 27, 1984

The author is with the Electronics Technology Division, Naval Research Laboratory, 4555 Overlook Ave., S. W., Washington, D C. 20375-5000.